5-2022

Compatible Blends of n-Type Polymer Semiconductors: Impact on the Morphology and Mechanics of Flexible Optoelectronics

Zachary C. Ahmad

Compatible Blends of n-Type Polymer Semiconductors: Impact on the Morphology and Mechanics of Flexible Optoelectronics

by

Zachary Chase Ahmad

A Thesis
Submitted to the Honors College of
The University of Southern Mississippi
in Partial Fulfillment
of Honors Requirements

May 2022

Approved by:

Xiaodan Gu, Ph.D., Thesis Advisor,
School of Polymer Science and Engineering

Derek Patton, Ph.D., Director,
School of Polymer Science and Engineering

Sabine Heinhorst, Ph.D., Dean
Honors College

ABSTRACT

Conjugated polymers offer the potential for the development of robust, low-cost electronics, but achieving high mechanical deformability and high charge transport simultaneously in polymer semiconductors remains a significant challenge. In this work, blends of conjugated polymers were investigated to elucidate the influence of compatible conjugated blends on polymer morphology, mechanics, and electrical properties (using a partially conjugated polymer as the soft matrix and a fully conjugated polymer as the electrically active component). This work achieves a fundamental understanding of blend morphology for these similar components by establishing the framework for how they deform with strain. Grazing-incidence wide-angle X-ray scattering (GIWAXS) was employed to investigate the crystalline morphology, atomic force microscopy (AFM) was used to monitor surface morphology, and organic thin film transistor devices were fabricated to understand the electrical properties. Additionally, blends of the conjugated polymers and polystyrene were compared to determine if the partially conjugated polymer is ultimately advantageous as the ductile component, i.e., promoting desired morphology for enhanced mechanics and electrical properties. The overall result of this work clarifies the use of flexible partially conjugated polymers as the matrix in blend systems and demonstrates a fundamental understanding of blend morphology for similar components.

Keywords: Flexible electronics, conjugated blends, X-ray scattering, morphology

DEDICATION

For the teachers who instilled in me the confidence to challenge my capabilities while equipping me with the knowledge that continues to change my life.

ACKNOWLEDGMENTS

It is with deep gratitude that I acknowledge my research advisor, Dr. Xiaodan Gu, who invested his time and his resources to my academic and professional development. His leadership sparked my love for research which continues to pave the road to my ambitions. I would like to thank my graduate mentor Luke Galuska who always treated me as an equal and taught me the importance of critical inquiry and clear communication. Through his mentorship, I gained the opportunity to pursue this work, along with countless others. I must thank the members of the Gu Research Group at large for their constant support and encouragement. Additionally, I would like to thank Dr. Jianguo Mei and his group from the Department of Chemistry at Purdue University for their collaboration and their synthesis of the primary materials used in this work.

I would like to thank the Honors College for the countless opportunities that matured my leadership skills, and Dean Heinhorst for providing constant support and encouragement in my pursuits. I can not express enough gratitude to the teachers and mentors at USM who made me a better scientist, such as Dr. Robson Storey, Dr. Julie Pigza, Dr. Derek Patton, and Emileigh McCardle. I must thank Dr. Heather Broadhead for providing the most constant support, encouragement, and influence during my undergraduate journey – she was the incontrovertible catalyst for so many of my successes. Additionally, I would like to thank my sister, Kailee, who always reminded me that my efforts were worthwhile. Finally, I wish to extend a special thanks to my friends, Zoe Gunter and Alyssa Necaise, who taught me how to be myself (a skill that has underlined every action I have taken in my years at USM).

TABLE OF CONTENTS

LIST OF TABLES

LIST OF ILLUSTRATIONS

LIST OF ABBREVIATIONS

AFM	Atomic Force Microscopy
CBS	Conjugation Break Spacer
Cx	Used to Denote a Carbon Spacer with a Varying (x) Number of Atoms
DPP	Diketopyrrolopyrrole
GIWAXS	Grazing-Incidence Wide-Angle X-ray Scattering
GPC	Gel Permeation Chromatography
IR	Infrared Spectroscopy
NMR	Nuclear Magnetic Resonance Spectroscopy
OFET	Organic Field Effect Transistor
P3HT	Poly(3-hexylthiophene-2,5-diyl)
PBTTT	Poly(2,5-bis(3- tetradecylthiophen-2-yl)thieno[3,2-b] thiophene)
PDMS	Polydimethylsiloxane
PNDI	Poly(Naphthalene-Diimide)-Based Polymers
PS	Polystyrene
PSS	Polystyrene Sulfonate
RPM	Revolutions Per Minute
T_g	Glass Transition Temperature
T_m	Melt Transition Temperature
$T_{operating}$	Operating Temperature
UV-Vis	Ultraviolet-Visible Spectroscopy

CHAPTER I: INTRODUCTION

Flexible electronics have gained increasing interest, both in the academic and industrial communities, owing to newfound applications within advanced soft robotics, prosthetics, and health monitoring technologies.[1,2,3,4] With the introduction of temperature signaling properties in polymeric materials, imparting skin-like sensing capabilities and stretchability to electronic devices can be accomplished by patterning traditional electronic materials or developing new intrinsically stretchable materials.[5] One remarkable property of skin is its ability to withstand the stress and strain of movement while still maintaining sensing functionality. This functionality relies on skin's ability to transmit electrical charges, which is the primary motivation for combining skin-like flexibility with charge mobility.

While cutting-edge applications of conductive elastic materials promise the availability of robust, low-cost electronics in the near future, achieving high mechanical deformability and high charge transport simultaneously in polymer semiconductors remains a significant challenge. Conjugated polymers are prime candidates for flexible technologies due to their high charge transport and mechanical compliance similar to biological tissue. Still, their intermolecular π-π stacking and high degree of fused aromatic rings result in highly rigid materials which are not favorable for mechanical deformability.[6] As a solution to this problem, the Gu and Mei research groups have successfully introduced compatible conjugation break spacers (CBS) - or linear alkyl chains - into the backbone of naphthalene diimide based conjugated polymers (PNDI) as a means to increase polymer flexibility and hence promote soft and ductile mechanical properties.[7] This design further provides a simple approach to modulating polymer

solution processability and offers a promising strategy to prepare melt-processable semiconducting polymers without the use of toxic and environmentally harmful solvents. These CBS-containing polymers have also been blended with a fully conjugated counterpart to provide enhanced electrical property.[8,9]

Though an understanding of the electrical properties of these blend materials has been achieved, applications are limited due to the lack of foundational information on the mechanical and morphological components of these blends.[10] To promote the widespread use of CBS materials, a comprehensive characterization of these blend systems must be conducted through morphological and conformational analysis methods. This work aims to study the effects of blend systems consisting of pure PNDI and PNDI with a 4-carbon CBS matrix on polymer morphology and, in turn, the morphology's impact on mechanical and electrical properties. This will result in the tunable optimization of the electrical contributions of the parent NDI polymer as well as the mechanical contributions afforded by a CBS matrix in a compatible blend system. Additionally, to determine if the partially conjugated polymer is ultimately beneficial as the ductile component, PNDI and polystyrene were blended for comparison since polystyrene (PS) has been widely studied and understood. To achieve these goals, tensile testing was employed to examine the mechanical performance of blend systems of varying PNDI concentration. Subsequently, their crystalline and surface morphology were investigated via grazing-incidence wide-angle X-ray scattering (GIWAXS) and atomic force microscopy (AFM), respectively, to provide further insight into the observed mechanical performance.

CHAPTER II: LITERATURE REVIEW

Conjugated polymers are macromolecules that possess alternating π and σ bonds along their molecular backbone, which renders them capable of transporting delocalized electrons. Along with their electron transporting capabilities, conjugated polymers have the potential for mechanical compliance, making them ideal candidates for flexible technologies. Conjugated polymers possess two modes of charge transport, intramolecular (along the conjugated backbone) and intermolecular transport (between π-stacked units). An example of modern diketopyrrolopyrrole (DPP) and isoindigo monomers that are commonly investigated for applications in organic field effect transistor (OFET) devices can be seen in Figure 1.

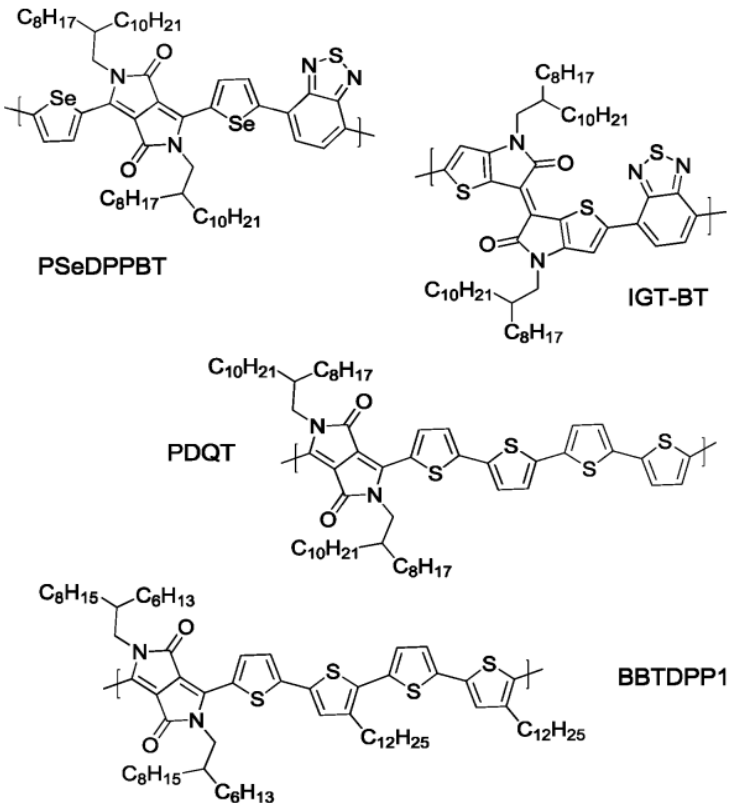

***Figure 1**. Common parent conjugated polymers.*[11]

The intermolecular π-π stacking in conjugated polymers results in the formation of highly crystalline domains, which is beneficial for high charge carrier mobility but renders conjugated polymer films brittle.[12] In this regard, conjugated break spacers (CBS), or linear alkyl chains, have been introduced into the backbone as a means to disentangle intramolecular and intermolecular transport effects and provide a simple approach to modulating polymer solution processability while also offering a promising strategy to prepare melt-processable semiconducting polymers.[13] For conjugated polymers with CBS incorporated randomly at small concentrations, the charge mobility was found to be largely maintained relative to the parent polymer, poly(2,5-bis(3-tetradecylthiophen-2-yl)thieno[3,2-b] thiophene) (PBTTT).[14] This can be attributed to the long-range percolation of conjugated units in a robust π-π network.

Recent developments in polymer research have provided a holistic perspective of the role of backbone flexibility on thin-film thermomechanics and morphology. In a recent study, Galuska *et al.* showed that the backbone flexibility of an n-type naphthalene diimide-based conjugated polymer (PNDI-Cx) (Figure 2) significantly increased upon addition of a CBS into the conjugated backbone.[4] This was made evident through the glass transition temperature (T_g), melting temperature (T_m), and elastic modulus which all demonstrated a reduction with increasing CBS length (Figure 3).

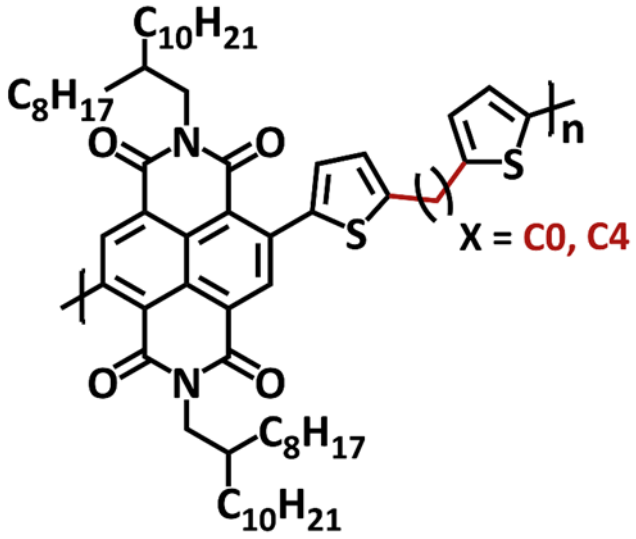

Figure 2. *Naphthalene diimide-based conjugated polymer (PNDI-Cx) with a pure C0 linkage and a C4 CBS linkage shown.*

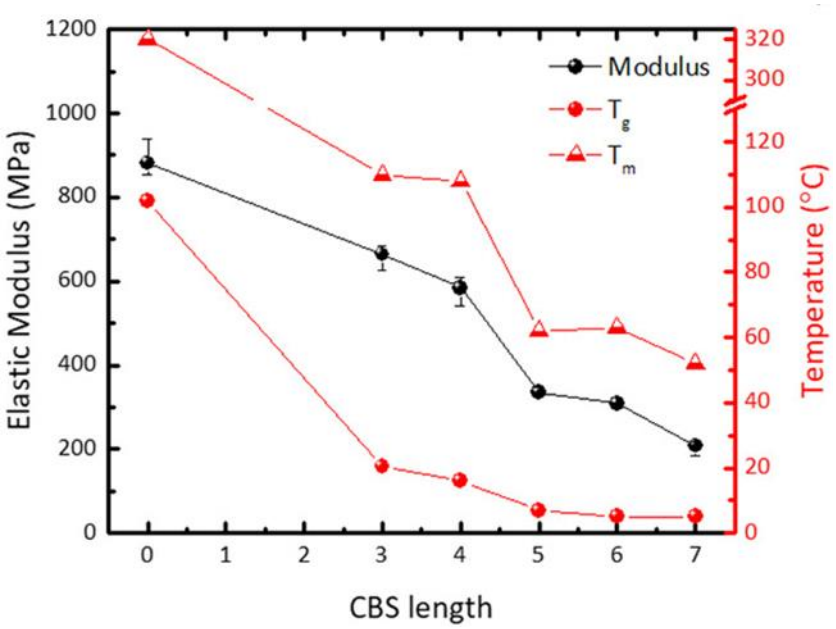

Figure 3. *Elastic modulus, backbone T_g, and T_m for examined PNDI-Cx polymers (Adapted with permission from ref 15. Copyright 2020 American Chemical Society).*[15]

Despite the high mechanical compliance upon insertion of CBS, intramolecular transport becomes hindered due to the loss in conjugation, resulting in reduced charge transport. Therefore, there remains a need to balance both mechanical and electrical properties. Previous studies have demonstrated the utility of blend systems containing CBS polymer as the matrix with as little as 2% fully conjugated polymer as the electrically active component, achieving near identical charge transport as the pure active component.[16]

For example, McNutt *et al.* detailed how the CBS PNDI polymer may be utilized in blend systems to promote melt-processability while also maintaining electrical charge transport.[15] In creating a complimentary semiconducting polymer blend (c-SPB) by blending a PNDI-C4 matrix with 5% fully conjugated poly[N,N′-bis(2-octyldodecyl)-1,4,5,8-naphthalenedicarboximide-2,6-diyl]-alt-5,5′-(2,2′-bithiophene) (P(NDI2OD-T2)), McNutt was able to examine electron mobility trends (Figure 4) and improve transistor performance up to 100-fold, relative to the pure PNDI-C4 matrix. Galuska and McNutt's studies provide a comprehensive inspiration for tailoring both physical and electrical properties of organic thin-film transistors with polymer blend systems. However, the mechanical compliance of such blend systems is currently unknown.

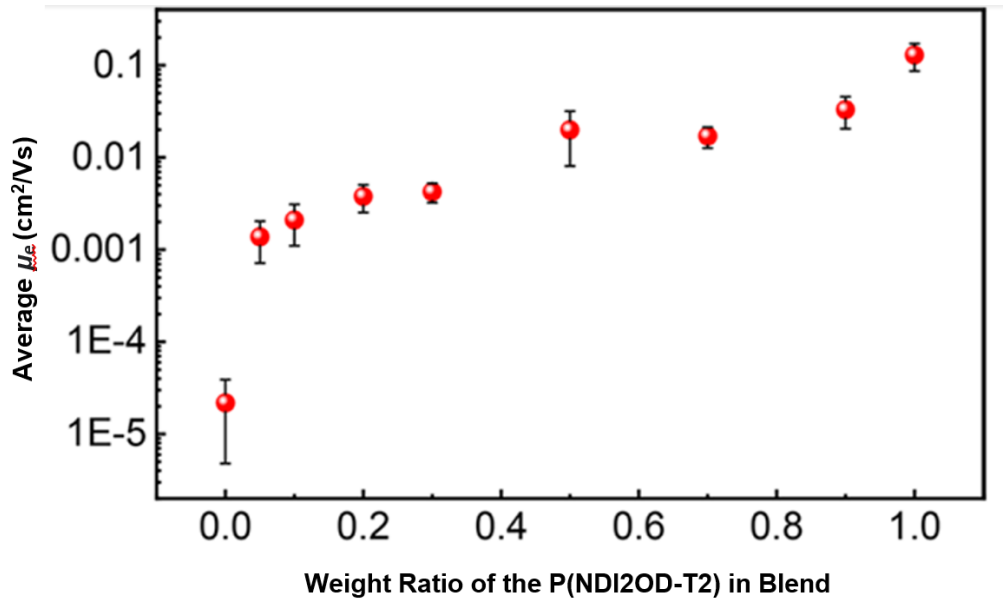

Figure 4. *N-type mobility trend for PNDI-C5 c-SPBs with increasing CBS length (Adapted with permission from ref 15. Copyright 2020 American Chemical Society).*[15]

The aim of this study is therefore to achieve both high ductility and electrical performance by blending the partially conjugated PNDI-C4, which displays high ductility, with the fully conjugated PNDI-C0, which displays high charge transport and compare with PNDI-C0/PS blends to determine if the C4 linker is advantageous as the ductile component. Resources from the lab of Jianguo Mei at Purdue University have been utilized to synthesize these polymers. Solutions were formulated, consisting of 2%, 5%, and 10% PNDI-C0 in chlorobenzene with PNDI-C4 as the primary component due to the expectation that the material will become more rigid as the concentration of C0 is increased. For the PNDI-C0/PS blends, the same formulations consisting of 2%, 5%, and 10% PNDI-C0 in chlorobenzene with PS as the primary component were followed. The efficacy of polymer blends in flexible electronic applications relies on their capability to

maintain a stable electric charge and their ability to exhibit robust mechanical properties.[17] The primary goal of this study was to maximize the electrical capacity in these materials by incorporating the lowest possible concentration of C0 while also maintaining the highest amount of ductility afforded by the PNDI-C4 matrix.

CHAPTER III: EXPERIMENTAL

Materials and Processing

Synthetic routes for the NDI-Cm polymers are shown in Figure 5. Linear methylene CBS monomers were synthesized using Stille coupling polymerization as reported in previous studies and the resulting polymers were then purified by sequential Soxhlet extraction with acetone, hexane, and chloroform. The hexane or chloroform fractions were collected, concentrated, and then precipitated in methanol.[18]

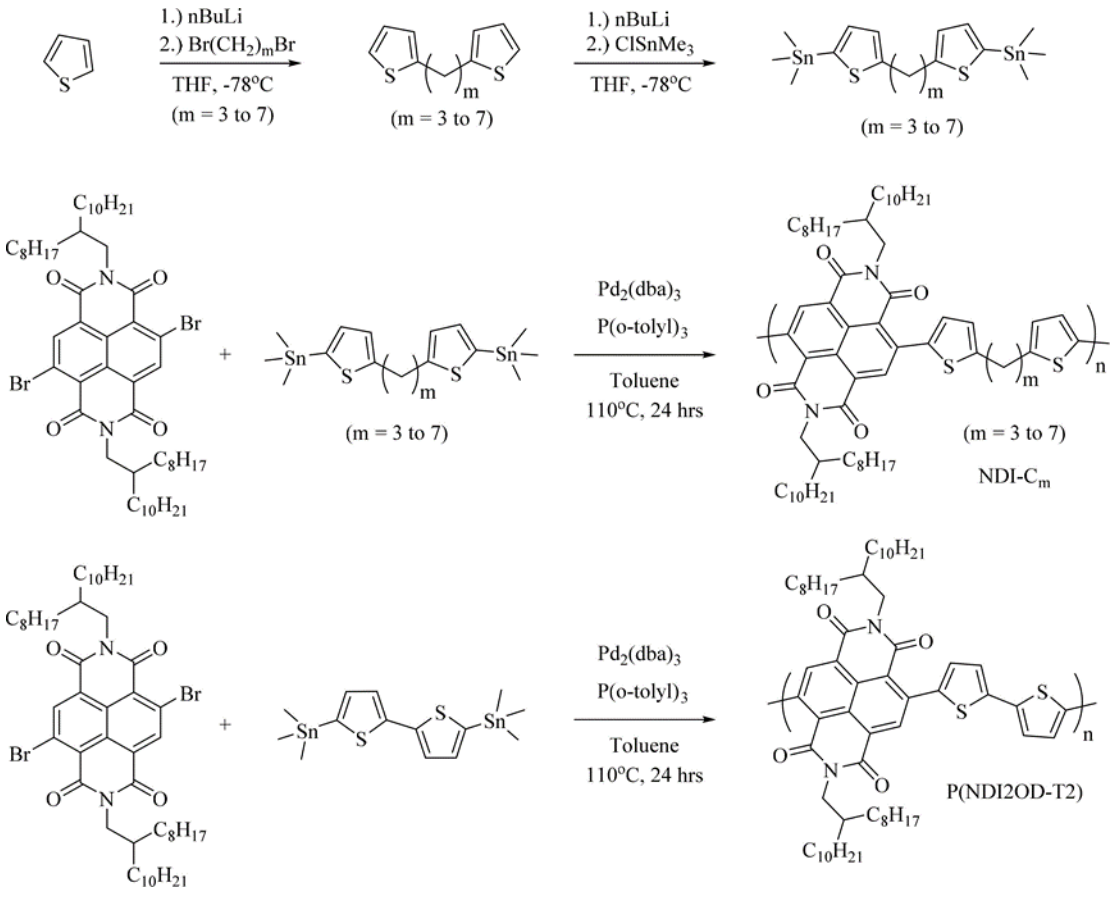

***Figure 5**. Synthesis of PNDI polymers.*[18]

The polymers were then collected via vacuum filtration and the relatively shorter spacers in this project were dried under vacuum and elevated temperatures. Longer spacers (5-7 carbon atom units) would require only vacuum due to the lower melting points with increased spacer length. As CBS length increased, the solubility of the PNDI polymers also increased (spacers containing more than 4 carbon atoms showed enhanced solubility in hexane) despite exhibiting molecular weights that were comparable to the polymers containing shorter CBS units. Following synthesis, the polymers were characterized by ^{1}H NMR spectroscopy and gel permeation chromatography (GPC) which confirmed the successful synthesis of the intended polymers.

Upon blending the respective counterparts, quantitative analysis was performed to understand how the two polymers interact to form a given morphology. After the solutions were prepared by dissolving the polymer in a chlorobenzene solvent at 18 mg/mL, they were fashioned into 60 μm (micrometer) thin films via spin-coating at a speed of 2000 rpm for 60 seconds. The samples were first spun cast onto a water soluble polystyrene sulfonate (PSS) layer. PSS solution is at 3% weight concentration in DI water and was spun cast at 4000 rpm for 60 seconds. Isothermal crystallization at room temperature occurs in PNDI-Cx polymers, which heightens the possibility of time-dependent mechanics for these materials since their morphology is in a steady state of flux (T_g < Toperating < T_m). Additionally, though the fully conjugated PNDI-C0 exhibits inherent crystallinity which cannot be obstructed (even when cooling from the melt stage at rates larger than 10,000 K/s), the heightened flexibility of the CBS systems results in relatively slow crystallization rates compared to the fully conjugated counterparts. Due to these considerations, an annealing protocol was designed to achieve equilibrated

morphologies for obtaining structure-property relationships without an obscure consideration of time dependence. Therefore, the polymers were annealed under a nitrogen atmosphere for two days prior to characterization, both at room temperature (25˚C) and at 30˚C below each polymer's individual T_m.

GIWAXS

In order to determine the mechanical properties of these blends and the potential for chain alignment upon stretching, GIWAXS analysis was performed on PNDI blends to monitor the crystalline morphology, and AFM analysis was performed to monitor surface morphology. GIWAXS is a scattering technique that allows for the investigation of the orientation and packing of the crystalline structures within thin film materials.

To understand how X-ray obtains this information, one may consider the semiconducting polymer P3HT as an example. P3HT is a common semiconducting polymer which crystallizes into the unit cell shown in Figures 6a and 6b. Following emission, the X-ray beam interacts with the sample and scatters which is recognized by a detector. The pattern then relays valuable information such as amount, size, and orientation of crystallites within the sample. Figure 6c displays the characteristic scattering signal of crystallites adopting an edge on orientation (Figure 6a). After comparing the materials in this experiment to similar materials from previous works, it was hypothesized that the PNDI polymers would shift from the face-on morphology (Figure 6b) to the edge-on orientation with increasing CBS content.[19]

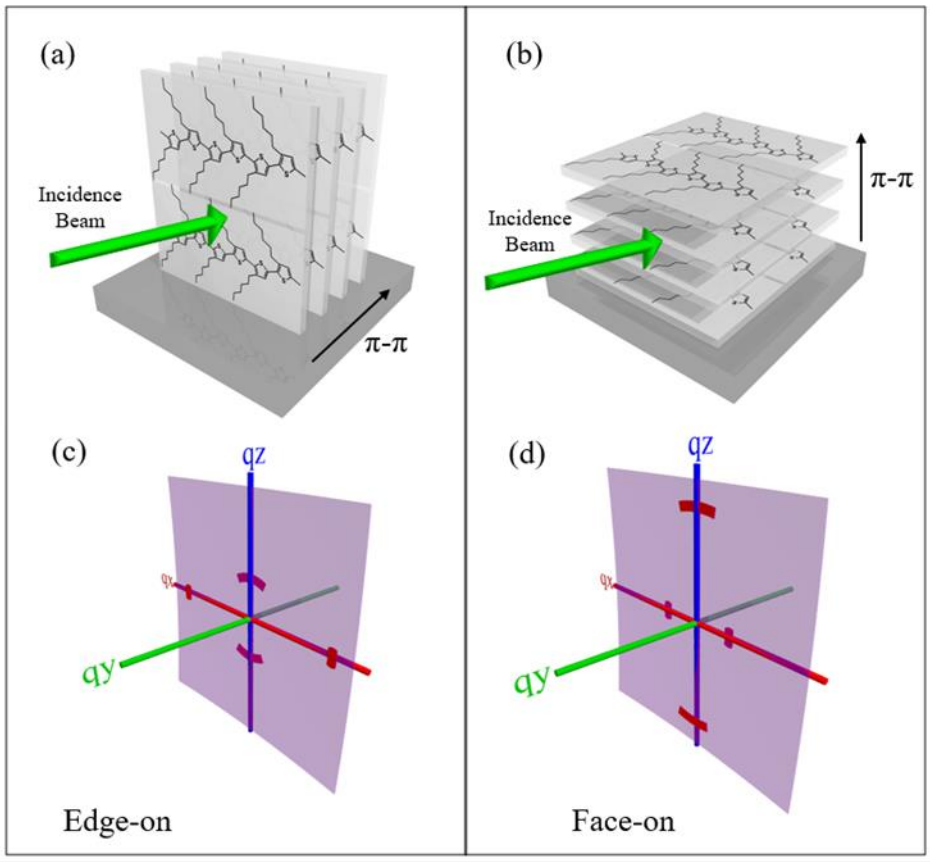

Figure 6. *(a) Edge-on oriented P3HT unit cell with π-π stacking in-plane. (b) Face-on oriented P3HT unit cell with lamellar stacking in-plane. (c) General scattering profile showing regions of interest in dark red for edge-on oriented P3HT. (d) General scattering profile showing regions of interest in dark red for face-on oriented P3HT (Adapted with permission from ref 20. Copyright 2020 Nature Communications).*[20]

The X-ray experiment in this work was performed on a Xenocs Xeuss 2.0 SAXS/WAXS lab source instrument. Diffraction analysis was completed using Nika software package within Wavemetrics Igor and WAXS tools. The samples were exposed for 2.5 hours to a incident beam energy of 8.05 keV, a beam geometry of 0.8 x 1.2 mm, an incidence angle of 0.2 degrees, and a sample to detector distance of approximately 157 mm.

Tensile Testing

Pseudo-free-standing tensile testing was performed following X-ray characterization by patterning the 60-µm thin-film blended samples of both PNDI-C0/C4 and PNDI-C0/PS into a dog-bone shape (gauge length of 8 mm and width of 2 mm) using a laser cutter and then floating the films on water before pulling unidirectionally at a strain rate of 5×10^{-4} s^{-1} until the film fractured. A schematic of this process is included in Figure 7.[21, 22]

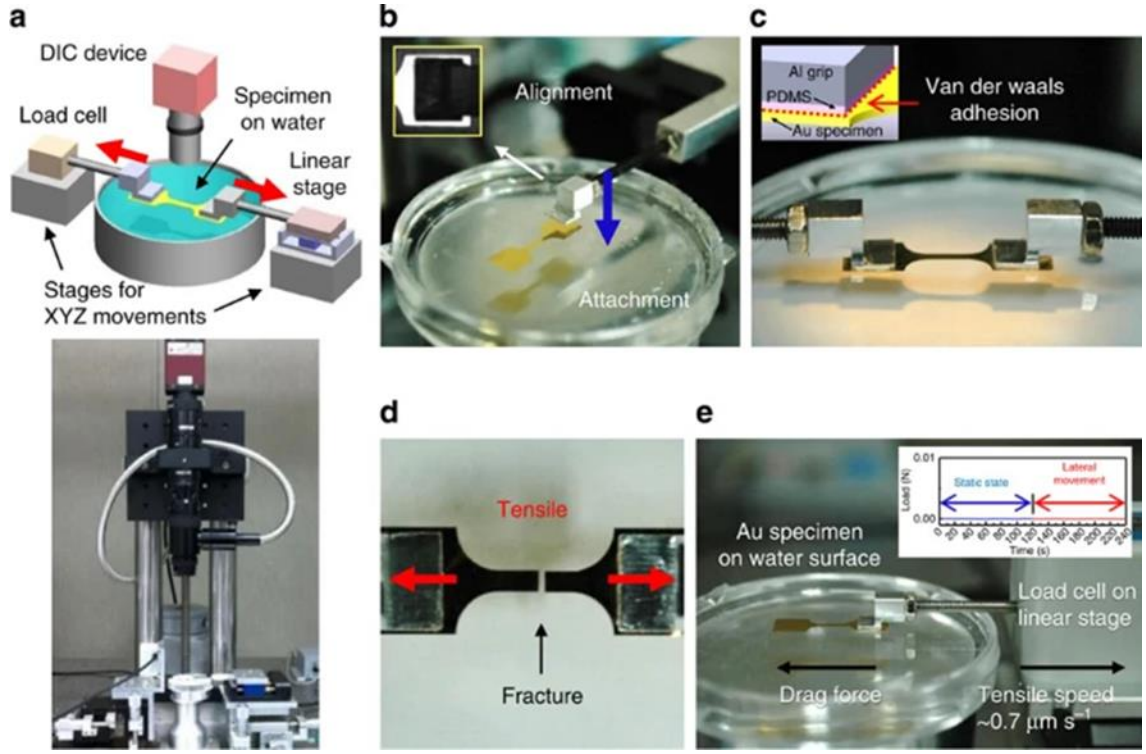

Figure 7*. Pseudo-free standing tensile testing. (a) Tensile testing system consisting of a load cell, linear stage, and DIC camera on an anti-vibration table. (b) An ultra-thin film afloat on the water surface with alignment and grip attachment via PDMS. (c) The ultra-thin Au film specimen being strongly gripped by van der Waals adhesion between the PDMS coating on the grips and the specimen surface. (d) Linear stage showing a fracture in the middle of the specimen's gauge length. (e) Drag force measurement made by attaching only one side of the specimen to the load cell connected to the linear stage (Adapted with permission from ref 22. Copyright 2018 Wiley).*[21, 22]

AFM

Atomic force microscopy (AFM), which is a microscopic technique that employs surface scanning to achieve images at nanoscale resolution, was then performed. Here, an Asylum Research Cypher S AFM was used, operating in AC mode in air, to investigate topographically and qualitatively how the blends organize to form a given morphology. Specifically, the information obtained via AFM was sought to support the arguments for or against phase separation for the blended materials in this work. The average thickness of the films was also obtained by AFM. AFM was performed by scratching the polymer film surface which was supported on a silicon wafer, and scanning the height difference between the bare silicon and the top of the film. The images of the systems in this study were collected post tensile strain atop a clean plasma etched silicon wafer after spin casting at a size scale of 30, 10, and 5 μm.

CHAPTER IV: RESULTS AND DISCUSSION

GIWAXS

Two primary representative chain packing directions that are orthogonal to each other can be extracted from the X-ray data obtained: (100) lamellar packing, which represents the distance between the alkyl side-chain regions; and (001) backbone chain packing, which represents the distance between two alternating electron donors/acceptors along a polymer backbone. A large amorphous halo (broad, unfocused circular ring seen for both samples in Figure 8a and 8b) was also observed for all the materials in this work, which previous works attribute to unoriented chain packing or an average of the intermolecular distances of amorphous chains.[23]

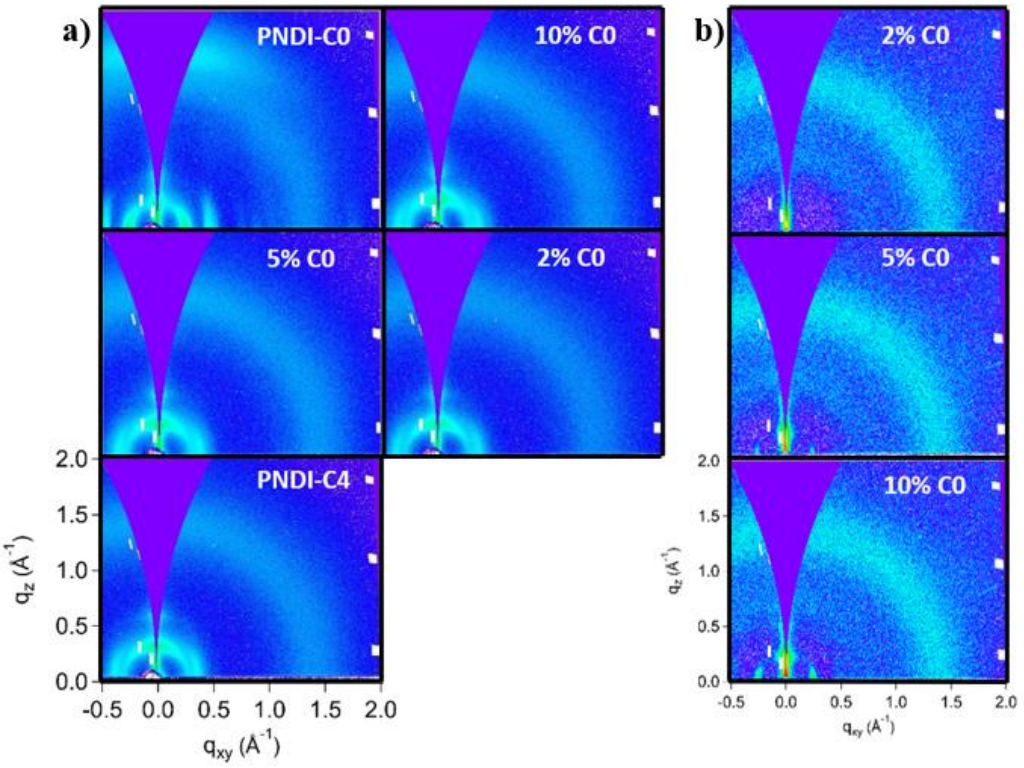

***Figure 8**. 2D GIWAXS profiles of **a)** PDNI-C0/C4 blends and **b)** PDNI-C0/PS blends.*

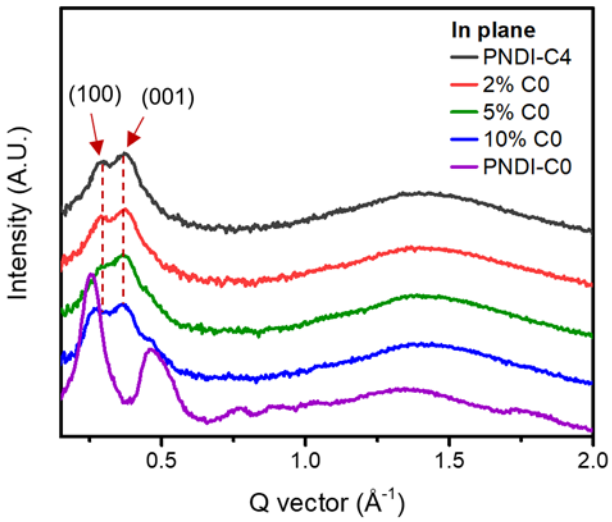

***Figure 9**. 1D GIWAXS scattering profiles of PNDI-C0/C4 blends.*

The 1D in-plane GIWAXS profile of the PNDI-C0/C4 blends is shown in Figure 9 relative to pure PNDI-C4 and PNDI-C0. As one can visually observe from the blend profiles, in appearance, they resemble the morphology of the pure PNDI-C4. An increase in the 001 peak (Q vector shift from 0.373 Å-1 to 0.473 Å-1) is observed which represents a decrease in the chain packing distance, for the fully conjugated PND-C0 polymer. Alternatively, a decrease of the 100 peak (Q vector shift from 0.291 Å-1 to 0.256 Å-1), was observed which signifies an increase in the alkyl packing distance for the fully conjugated PND-C0 polymer. The absence of a clearly distinguishable 010 (π-π stacking) peak among the data reveals that the blends do not possess π-π stacking and demonstrates co-crystallization, which favors the CBS containing matrix polymer over the C0 counterpart. Upon addition of CBS, a slight shift from the face-on to edge-on morphology (Table 1) was also observed. The values for the shifts in These findings suggest that both the C0 pure component and the C4 matrix both act as semiconductors (with C4 being more flexible than C0) and both exhibit regions of crystallinity.

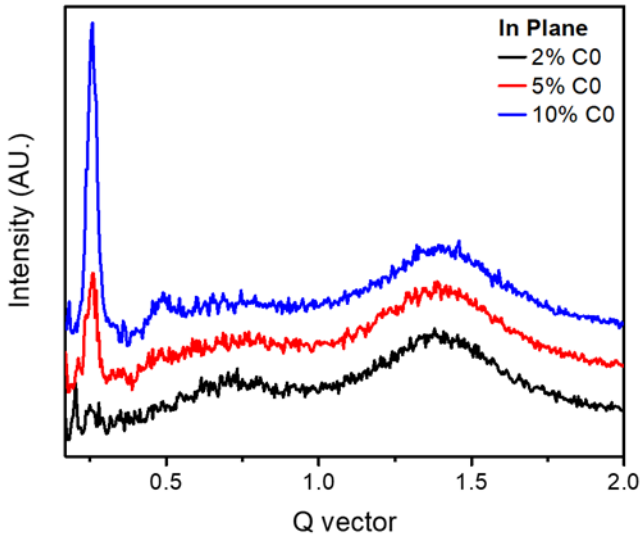

***Figure 10**. 1D GIWAXS scattering profiles of PDNI-C0/PS blends.*

For the PS blends seen in Figure 10, regardless of how much C0 concentration is incorporated, the blends favor the morphology of the PS which is a highly amorphous (lacking structural order) material with relatively low scattering signal. This suggests that PS acts as an insulator which will interrupt the electron flow. The values for Q vector of both PS and NDI blends are included in Table 1.

Table 1. Peak values for GIWAXS spectra in Angstroms ($Å^{-1}$).

NDI/NDI Blends	**100 Peak ($Å^{-1}$)**	**001 Peak ($Å^{-1}$)**
PNDI-C4	0.291	0.373
2% C0	0.291	0.375
5% C0	0.289	0.379
10% C0	0.272	0.379
PNDI-C0	0.256	0.473
NDI/PS Blends	**100 Peak ($Å^{-1}$)**	**001 Peak ($Å^{-1}$)**
2% C0	0.253	-
5% C0	0.265	0.456
10% C0	0.257	0.485

Tensile Testing

The tensile data for PNDI-C4 (Figure 12a) displays a shortened strain before fracture as more of the fully conjugated polymer is introduced. Despite this trend, the strain prior to failure remains exceedingly high at 150% compared to C0 at less than 10%. The tensile data in Figure 11a shows that the C4 blend maintains ductility at high levels of fatigue, stretching up to 400% strain. It can be seen that the modulus is not greatly impacted by the matrix but the C0 component does act as a source of defect for strain. For the PS blends (Figure 11b), the data shows a much higher modulus than C4 blends before fracture. These materials are much less ductile and much more resistant to deformation before fracturing.

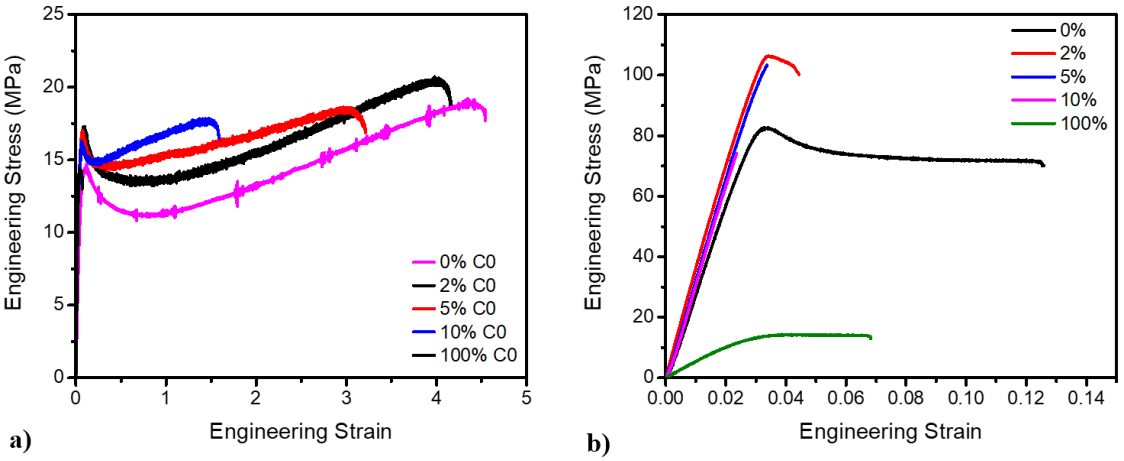

Figure 11*. Tensile data for* ***a)*** *PNDI-C0/C4 blends and* ***b)*** *PNDI-C0/PS blends.*

As can be concluded from the modulus vs concentration graph for PNDI-C0/C4 (Figure 12a), the materials are inversely proportional, meaning that they are complementary, and that whichever material is in the majority will dictate the properties. For the PS blend (Figure 12b), PNDI initially constricts movement of the PS, but

increasing the content of PNDI causes phase separation and PNDI conglomerates. Phase separation is a negative attribute in this case since it means that the space where electrons could flow is increased thereby dampening the electrical conductivity. The advantage of PNDI-C4 over PS is that its chains will align as it stretches.

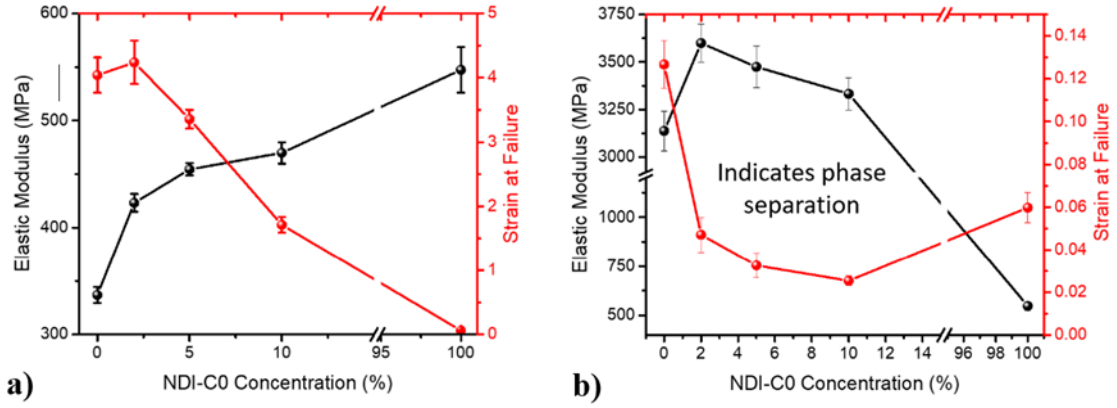

***Figure 12**: Mechanical properties vs concentration graphs of **a)** PNDI-C0/C4 and **b)** PNDI-CO/PS.*

AFM

As can be seen from the collected AFM images for PNDI-C0/C4 blends (Figure 13), the blend system gave rise to a floral-type pattern. Bright and dark regions are observed which represent the individual components, but it is difficult to pinpoint where the regions begin or end. Their heavy intertwinement suggests a more optimal amalgamated phase which will contribute to the electron mobility of the material. If these images suggest that PNDI-C0 is forming into non-connected tubular aggregates intertwined with the PNDI-C4 chain, then this suggestion agrees with our findings from

GIWAXS. When observing the images for PS blends (Figure 14), one can see clearly differentiable phases, as the dark bands are isolated from the lighter regions. This once again suggests phase separation which dampens electrical conductivity.

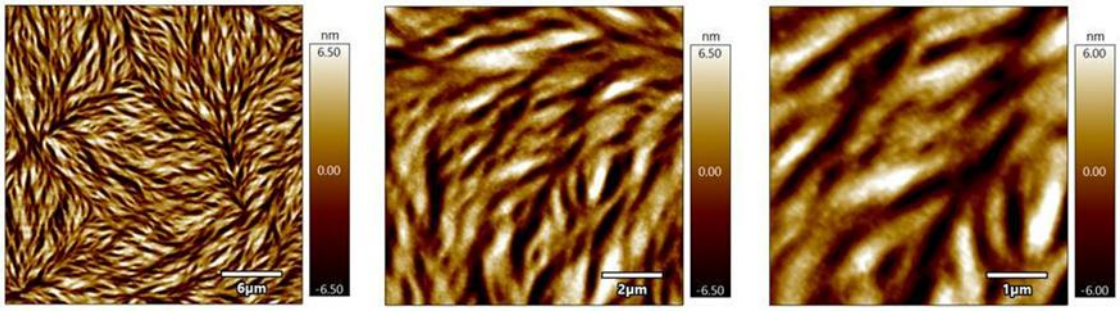

Figure 13. *AFM images of PNDI-C0/C4 blends, taken at 30 µm, 10 µm, and 5 µm.*

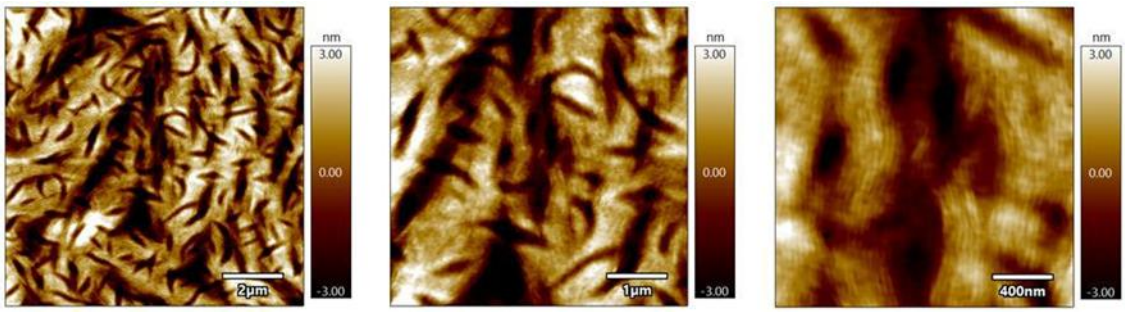

Figure 14. *AFM images of PNDI-C0/PS blends, taken at 10 µm, 5 µm, and 2000 nm.*

Given the similarity between PNDI-C0 and PNDI-C4, there is a potential challenge in distinguishing the contribution of each component towards the morphology. Deuterated polymers have a specific infrared absorption which can provide a clear distinction between the two polymers in question within a given AFM image. Therefore, it is possible to distinguish the morphology of the two components by deuteration of the C4 linker in conjunction with AFM-IR. A deuterated polymer phase can be clearly differentiated from a non-deuterated polymer based on non-overlapping infrared (IR)

stretching vibrations of their carbon−hydrogen and carbon−deuterium alkyl chains (C−D stretch 2000−2250 cm−1; C−H stretch, 2800−3050 cm−1).[24] X-ray photoelectron spectroscopy will also be employed to determine if the polymers vertically phase segregate vs segregating throughout the thickness of our film, and polarized ultraviolet-visible (UV-Vis) spectroscopy to monitor the chain backbone alignment throughout tensile deformation.

CHAPTER V: CONCLUSION

In summary, PNDI-C0/C4 blends are complimentary, meaning that whichever material is in the majority will dictate the properties of the final product. For example, increase of PNDI-C0 content in the blend will increase electrical properties but at the expense of some mechanical resilience as afforded by the PNDI-C4 matrix. PDNI-C0/PS are non-complimentary, since the PNDI-C0 component is more ductile than the overall blends and its modulus is lower than that of polystyrene. This indicates poor ductility and phase separation of the PS blend as is supported by AFM. PNDI-C0 then, acts as a semiconductor and PNDI-C4 is its flexible semiconducting counterpart, whereas PS would act as an insulator.

This work serves to establish the use of flexible partially conjugated polymers as the ductile matrix in blend systems to reach a fundamental understanding of blend morphology for like components. The research in this project will be expanded further as a comprehensive suite of characterization methods will be provided that will either confirm or deny the use of PNDI blend systems in widespread flexible organic electronic applications. This study proves invaluable to the field of biomimetics and prosthetics, as well as optoelectronic devices where the need for soft, ductile electronics is paramount. Additionally, the polymers in this study are melt-processable which eliminates the need for toxic solvents. This is of paramount importance as polymer scientists continue to integrate more environmentally friendly processing methods into everyday use.

REFERENCES

1. Song, J.; Kim, M.; Yoo, S.; Koo, J.; Kim, D. Materials and Devices for Flexible and Stretchable Photodetectors and Light-Emitting Diodes. *Nano Research* **2021**, *14*, 2919–2937.
2. Wang, S.; Xu, J.; Wang, W.; Wang, G.-J. N.; Rastak, R.; Molina-Lopez, F.; Chung, J. W.; Niu, S.; Feig, V. R.; Lopez, J.; et al. Skin Electronics from Scalable Fabrication of an Intrinsically Stretchable Transistor Array. *Nature* **2018**, *555*, 83–88.
3. Someya, T.; Bao, Z.; Malliaras, G. G. The Rise of Plastic Bioelectronics. *Nature* **2016**, *540*, 379–385.
4. Someya, T.; Bauer, S.; Kaltenbrunner, M. Imperceptible Organic Electronics. *MRS Bull*. **2017**, *42*, 124–130.
5. Chortos, A.; Bao, Z. Skin-Inspired Electronic Devices. *Mater. Today*. **2014**, *17*, 321–331.
6. Liu, D.; Mun, J.; Chen, G.; Schuster, N. J.; Wang, W.; Zheng, Y.; Nikzad, S.; Lai, J.-C.; Wu, Y.; Zhong, D.; Lin, Y.; Lei, Y.; Chen, Y.; Gam, S.; Chung, J. W.; Yun, Y.; Tok, J. B.-H.; Bao, Z. A Design Strategy for Intrinsically Stretchable High-Performance Polymer Semiconductors: Incorporating Conjugated Rigid Fused-Rings with Bulky Side Groups. *J. Am. Chem. Soc*. **2021**, *143*, 11679–11689.
7. Galuska, L. A.; McNutt, W. W.; Qian, Z.; Zhang, S.; Weller, D. W.; Dhakal, S.; King, E. R.; Morgan, S. E.; Azoulay, J. D.; Mei, J.; Gu, X. Impact of Backbone Rigidity on the Thermomechanical Properties of Semiconducting Polymers with Conjugation Break Spacers. *Macromolecules* **2020**, *53*, 6032–6042.

8. Zhao, Y.; Zhao, X.; Roders, M.; Qu, G.; Diao, Y.; Ayzner, A. L.; Mei, J. Complementary Semiconducting Polymer Blends for Efficient Charge Transport. *Chem. Mater*. **2015**, *27*, 7164–7170.

9. Zhao, Y.; Zhao, X.; Zang, Y.; Di, C.-A.; Diao, Y.; Mei, J. Conjugation-Break Spacers in Semiconducting Polymers: Impact on Polymer Processability and Charge Transport Properties. *Macromolecules* **2015**, *48*, 2048–2053.

10. Wu, Y.; Schneider, S.; Walter, C.; Chowdhury, A. H.; Bahrami, B.; Wu, H.-C.; Qiao, Q.; Toney, M. F.; Bao, Z. Fine-Tuning Semiconducting Polymer Self-Aggregation and Crystallinity Enables Optimal Morphology and High-Performance Printed All-Polymer Solar Cells. *J. Am. Chem. Soc*. **2020**, *142*, 392–406.

11. Holliday, S.; Donaghey, J. E.; McCulloch, I. Advances in Charge Carrier Mobilities of Semiconducting Polymers Used in Organic Transistors. *Chem. Mater.* **2014**, *26*, 647–663.

12. Ashizawa, M.; Zheng, Y.; Tran, H.; Bao, Z. Intrinsically Stretchable Conjugated Polymer Semiconductors in Field Effect Transistors. *Prog. Polym. Sci*. **2020**, *100*, 101181.

13. Melenbrink, E. L.; Hilby, K. M.; Choudhary, K.; Samal, S.; Kazerouni, N.; McConn, J. L.; Lipomi, D. J.; Thompson, B. C. Influence of Acceptor Side-Chain Length and Conjugation-Break Spacer Content on the Mechanical and Electronic Properties of Semi-Random Polymers. *ACS Appl. Polym. Mater*. **2019**, *1*, 1107–1117.

14. Pathiranage, T. M. S. K.; Dissanayake, D. S.; Niermann, C. N.; Ren, Y.; Biewer, M. C.; Stefan, M. C. Role of Polythiophenes as Electroactive Materials. *J. Polym. Sci*. *A Polym. Chem*. **2017**, *55*, 3327–3346.

15. McNutt, W. W.; Gumyusenge, A.; Galuska, L. A.; Qian, Z.; He, J.; Gu, X.; Mei, J. N-Type Complementary Semiconducting Polymer Blends. *ACS Appl. Polym. Mater*. **2020**, *2*, 2644–2650.

16. Zhao, X.; Zhao, Y.; Ge, Q.; Butrouna, K.; Diao, Y.; Graham, K. R.; Mei, J. Complementary Semiconducting Polymer Blends: The Influence of Conjugation-Break Spacer Length in Matrix Polymers. *Macromolecules* **2016**, *49*, 2601–2608.

17. Rong, Q.; Lei, W.; Liu, M. Conductive Hydrogels as Smart Materials for Flexible Electronic Devices. *Chemistry* **2018**, *24*, 16930–16943.

18. Qian, Z.; Galuska, L. A.; Ma, G.; McNutt, W. W.; Zhang, S.; Mei, J.; Gu, X. Backbone Flexibility on Conjugated Polymer's Crystallization Behavior and Thin Film Mechanical Stability. *J. Poly. Sci*. **2022**, *60*, 548–558.

19. Lin, Y.-C.; Matsuda, M.; Chen, C.-K.; Yang, W.-C.; Chueh, C.-C.; Higashihara, T.; Chen, W.-C. Investigation of the Mobility–Stretchability Properties of Naphthalenediimide-Based Conjugated Random Terpolymers with a Functionalized Conjugation Break Spacer. *Macromolecules* **2021**, *54*, 7388–7399.

20. GISAXS for Thin Film Polymer Characterization [Online]; http://www.cei.washington.edu/education/science-of-solar/gisaxs-for-thin-film-polymer-characterization/ (accessed Nov 4, 2022).

21. Kim, J.-H.; Nizami, A.; Hwangbo, Y.; Jang, B.; Lee, H.-J.; Woo, C.-S.; Hyun, S.; Kim, T.-S. Tensile Testing of Ultra-Thin Films on Water Surface. *Nat. Commun*. **2013**, *4*, 2520.

22. Zhang, S.; Ocheje, M. U.; Luo, S.; Ehlenberg, D.; Appleby, B.; Weller, D.; Zhou, D.; Rondeau-Gagné, S.; Gu, X. Probing the Viscoelastic Property of Pseudo Free-Standing Conjugated Polymeric Thin Films. *Macromol. Rapid Commun*. **2018**, *39*, e1800092.

23. Zhang, S.; Alesadi, A.; Mason, G. T.; Chen, K.-L.; Freychet, G.; Galuska, L.; Cheng, Y.-H.; St. Onge, P. B. J.; Ocheje, M. U.; Ma, G.; Qian, Z.; Dhakal, S.; Ahmad, Z.; Wang, C.; Chiu, Y.-C.; Rondeau-Gagné, S.; Xia, W.; Gu, X. Molecular Origin of Strain-induced Chain Alignment in PDPP-based Semiconducting Polymeric Thin Films. *Adv. Funct. Mater*. **2021**, *31*, 2100161.

24. Painter, P.; Zhao, H.; Park, Y. Infrared Spectroscopic Study of Thermal Transitions in Poly(Methyl Methacrylate). *Vib. Spectrosc*. **2011**, *55*, 224–234.